Spectral properties of multiorder diffractive lenses

Dean Faklis and G. Michael Morris

Diffractive lenses have been traditionally designed with the first diffracted order. The spectral characteristics of diffractive lenses operating in higher diffracted orders differ significantly from the first-order case. Multiorder diffractive lenses offer a new degree of freedom in the design of broadband and multispectral optical systems that include diffractive optical elements. It is shown that blazing the surface-relief diffractive lens for higher diffraction orders enables the design of achromatic and apochromatic singlets. The wavelength-dependent optical transfer function and the associated Strehl ratio are derived for multiorder diffractive lenses. Experiments that illustrate lens performance in two spectral bands are described, and the results show excellent agreement with the theoretical predictions.
Key words: Diffractive optics, binary optics, optical design, optical testing, kinoforms.

1. Introduction

Diffractive optics offers optical system designers new degrees of freedom that can be used to optimize the performance of optical systems. The zone spacing of a diffractive lens can be chosen to impart focusing power as well as aspheric correction terms to the emerging wave front. The surface (or blaze) profile within a given zone determines the diffraction efficiency of the element or, in other words, determines how the incident energy is distributed among the various diffraction orders.

The basic structure of a diffractive lens is illustrated in Fig. 1. Figure 1(a) shows a portion of a refractive lens. By removing the multiple 2π phase delays from the refractive lens, one obtains a diffractive lens, as shown in Fig. 1(b), i.e., one can think of a diffractive lens as a modulo 2π lens.[1,2] The blaze profile within each zone of the diffractive lens provides perfect constructive interference at the focal plane for the design wavelength λ_0 (i.e., the wavelength that experiences a 2π phase jump at each zone boundary). Figures 1(c) and 1(d) illustrate different approximations to the desired blaze profile in Fig. 1(b). The blaze profile shown in Fig. 1(b) can be produced by, for example, laser pattern generation or single-point diamond turning.[3] The discrete-step blaze profile shown in Fig. 1(d) can be produced by an N-step photolithographic process,[4] in which N denotes the number of photomasks that is used (the number of phase steps per zone is equal to 2^N). The zone radii, r_j, are obtained by the solution of the equation, $\phi(r_j) = 2\pi j = s_1 r_j^2 + s_2 r_j^4 + s_3 r_j^6 + \ldots$, where $\phi(r)$ represents the desired phase of the wave front emerging from the element at radius r from the optical axis. The phase coefficient, s_1, determines the optical (or focusing) power of the element. The phase coefficients, s_2, s_3, etc., determine the aspheric contributions to the wave front. In a given application, the phase coefficients can be optimized by the use of commercial lens-design software.

Although it is often useful to think of a diffractive lens as a modulo 2π lens at the design wavelength, the spectral properties (or wavelength dependence) of a diffractive lens are drastically different from those of a refractive lens. For a thin refractive lens [Fig. 1(a)], the lens power is given by $\Phi(\lambda) = [n(\lambda) - 1]c$, where $n(\lambda)$ denotes the index of refraction of the lens material at wavelength λ and c represents the surface curvature of the lens, whereas, for a diffractive lens [Figs. 1(b)–1(d)], the optical power (associated with the r^2 phase term) is highly wavelength dependent. In fact, the optical power varies linearly with the wavelength of light, i.e., $\Phi(\lambda) = \lambda/[\lambda_0 F(\lambda_0)]$. The dispersion of a diffractive lens is roughly 7 times larger than the strongest flint glass currently available and is opposite in sign. In the design of broadband optical systems, diffractive lenses that have the proper optical power can be used to replace refractive lenses in the system, which generally provides a

The authors are with the Rochester Photonics Corporation, 330 Clay Road, Rochester, New York 14623. G. M. Morris is also with the Institute of Optics, University of Rochester, Rochester, New York.

Received 6 September 1994; revised manuscript received 18 November 1994.

0003-6935/95/142462-07$06.00/0.

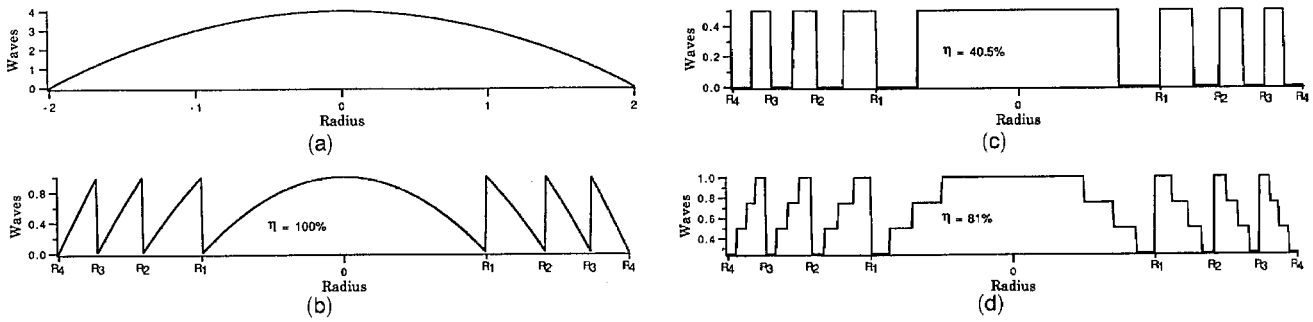

Fig. 1. Diffractive lens construction: (a) conventional refractive lens, (b) diffractive lens with continuous quadratic blaze profile, (c) phase-reversal (or Wood) lens, (d) four-level approximation to quadratic blaze profile.

significant reduction in the weight and the number of optical elements required for achieving a specified level of performance.[5]

In this paper we investigate the spectral properties of multiorder diffractive (MOD) lenses.[6] A MOD lens differs from the standard diffractive lenses described above in that the phase jump at the zone boundaries is taken to be a multiple of 2π, i.e., $\phi(r_j) = 2\pi p$, where p is an integer ≥ 2, and the location of the zone radii are obtained by the solution of the equation $\phi(r_j) = 2\pi pj$, where again $\phi(r)$ represents the phase function of the emerging wave front. The number of 2π phase jumps, p, represents a degree of freedom for the designer. However, to date, most of the reported investigations with diffractive lenses have set $p = 1$, by default.

In the literature there are only a few articles that consider MOD (or higher-order diffractive) lenses. In a footnote, Miyamoto[1] states that one can reduce the problems associated with small zone spacings by using multiple 2π phase jumps at the zone boundaries. He writes, "This type (of lens) is more easily produced because the width of each Fresnel zone becomes broader; however, the effect of the discontinuities in the wave surface of the different wavelength becomes more serious than that of the original PFL (phase Fresnel lens)." Dammann[7,8] considered the spectral characteristics of stepped-phase gratings that have an arbitrary phase jump at the edge of each grating facet and the application of these gratings for color separation.

Futhey[9] and Futhey *et al.*[10] have described what they call a "super-zone" diffractive lens. The structure of a super-zone lens is, again, motivated by the desire to keep the zone spacing of the various facets above the resolution limit imposed by the particular fabrication method (diamond turning, laser pattern generation, or photolithography). In the center of a super-zone lens, p is typically set equal to 1. As the radial distance from the center of the lens increases, the zone spacing gets closer together. When the zone spacing begins to approach the limits of resolution of the fabrication method, one then changes phase jumps at the zone boundaries to $2\pi p$, where p is now set equal to, say, 2 or 4. When the zone spacings again begin to approach the limits of resolution of the fabrication method, one again increases the value of p, and repeats this procedure until the desired radius for the lens element is obtained.

Marron *et al.*[11] have also reported on "higher-order kinoform" structures. The motivation for their work was, again, to keep surface features large compared with the wavelength of light, even when the f-number of the lens is very low.

Sweeney and Sommargren[12] investigated the application of higher-order diffractive lenses and they generated an $f/7$ acrylic lens with a focal length of 40 mm. The design wavelength was 550 nm and $p = 20$, which gives a maximum surface-relief depth of approximately 23 μm. The master element was diamond turned in aluminum, and Sweeney and Sommargren presented qualitative description of imaging performance. There were a total of 14 zones across the clear aperture.

Although it is important to realize that the larger zone structure of a MOD lens is easier to produce than that of a standard modulo 2π diffractive lens, we have found the spectral properties of MOD lenses to be particularly interesting and useful. For example, as we show in Section 2, one can form either an achromatic or an apochromatic diffractive singlet by choosing the appropriate value for p. Such elements may be particularly useful in color image displays.[13]

In Section 2, we consider the first-order properties of MOD lenses, namely, the optical power, the diffraction efficiency, and the structure of achromatic and apochromatic diffractive singlets. In Section 3, the imaging properties of MOD lenses are described, including a discussion of the optical transfer function (OTF) for a MOD lens and the wavelength dependence of the Strehl ratio. To demonstrate the spectral properties experimentally, we fabricated a MOD lens by using a single-point laser pattern generator (LPG). The experimental performance of the MOD lens is contained in Section 4.

2. First-Order Properties of Paraxial Multiorder Diffractive Lenses

In this section, the first-order properties of paraxial MOD lenses are presented within the framework of scalar diffraction theory. We start by describing the amplitude transmission function of the diffractive

singlet. The construction of the diffractive zone structure for Fresnel full-period zones is defined such that the optical path difference across the jth zone is equal to $(F_0 + jp\lambda_0)$, where λ_0 is the design wavelength, F_0 is the focal length when the illumination wavelength $\lambda = \lambda_0$, and p is an integer that represents the maximum phase modulation as a multiple of 2π. In the paraxial region, the locations of the zones in the plane of the lens are given by

$$r_j^2 = 2jp\lambda_0 F_0. \tag{1}$$

The optical phase introduced by the diffractive element is given by[14]

$$\phi(r) = 2\pi\alpha p\left(j - \frac{r^2}{2p\lambda_0 F_0}\right), \qquad r_j \le r < r_{j+1}, \tag{2}$$

where α is defined as the fraction of 2π phase delay that is introduced for illumination wavelengths other than the design wavelength and is given by

$$\alpha = \frac{\lambda_0}{\lambda}\left[\frac{n(\lambda) - 1}{n(\lambda_0) - 1}\right], \tag{3}$$

where n is the index of refraction of the material in the grating region. The maximum height of the surface relief is given by

$$h_{\max}(r) = \frac{p\lambda_0}{n(\lambda_0) - 1}. \tag{4}$$

In a manner similar to that used in Ref. 14, the amplitude transmission function of the diffractive lens can be expanded as a Fourier series to give

$$t(r) = \sum_{m=-\infty}^{\infty} \exp[-i\pi(\alpha p - m)] \times \operatorname{sinc}(\alpha p - m)\exp\left(-\frac{i\pi m r^2}{p\lambda_0 F_0}\right), \tag{5}$$

where $\operatorname{sinc}(x) = \sin(\pi x)/(\pi x)$ and m denotes the mth diffraction order. It is important to note that the transmission function in Eq. (5) represents a diffractive lens within the paraxial approximation and that transmission functions that describe other diffractive lenses (e.g., anamorphic or aspheric) are possible. It is interesting to compare Eq. (5) with the transmission function of a conventional refractive lens[15] given by

$$t(r) = \exp\left(-\frac{i\pi r^2}{\lambda F}\right), \tag{6}$$

where F is the focal length, which depends on the material properties of the lens. A comparison of Eqs. (5) and (6) suggests that there are an infinite number of focal lengths given by

$$F(\lambda) = \frac{p\lambda_0 F_0}{m\lambda}. \tag{7}$$

Note that the focal length in Eq. (7) is proportional to p and inversely proportional to the illumination wavelength and the diffraction order, m. It is interesting to note that when the quantity in Eq. (7), $p\lambda_0/m\lambda$, is set equal to unity, several wavelengths within a given band can come to a common focus. Clearly p is a construction parameter and is usually constant across the lens radius, and the wavelengths that are focused to a common point are chosen from a set of diffraction orders (i.e. MOD lenses). Although a diffractive lens with a maximum phase modulation of 2π can allow a mutual focus for simple harmonics of the design wavelength, the parameter p now offers a mechanism to control specific wavelengths in a given band or bands that will come to a fixed focus. This property allows the design of achromats and apochromats by the use of a single diffractive surface.

The scalar diffraction efficiency, η_m, of the mth diffracted order is given by the squared modulus of its Fourier coefficient in Eq. (5), i.e.,

$$\eta_m = \operatorname{sinc}^2(\alpha p - m). \tag{8}$$

The diffraction efficiency given by Eq. (8) is unity when the argument of the sinc function is equal to 0. Note that this condition can allow for high diffraction efficiency for several wavelengths. For example, consider the case of a MOD lens operating in the visible region with $p = 10$. Figure 2 illustrates the wavelength dependence of the diffraction efficiency for a range of diffracted orders, with material dispersion neglected. The peaks in diffraction efficiency occur at precisely those wavelengths that come to a common focus [see Eq. (7)], i.e.,

$$\lambda_{\text{peak}} = \frac{p\lambda_0}{m}. \tag{9}$$

It is important to note a well-known property of operation when higher diffracted orders are used.

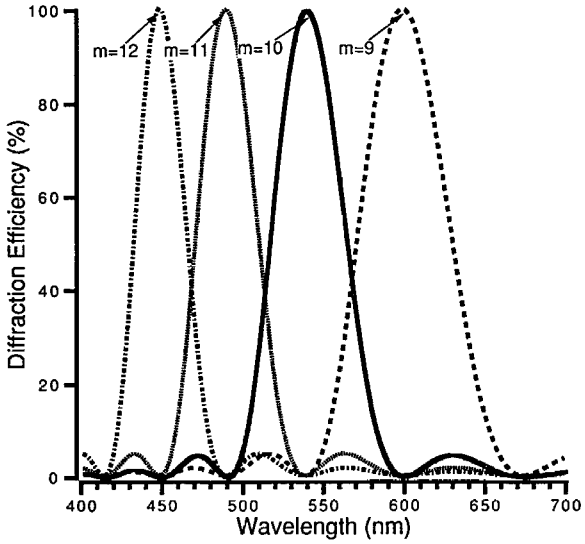

Fig. 2. Diffraction efficiency of the mth diffracted order versus wavelength for a MOD lens with $p = 10$.

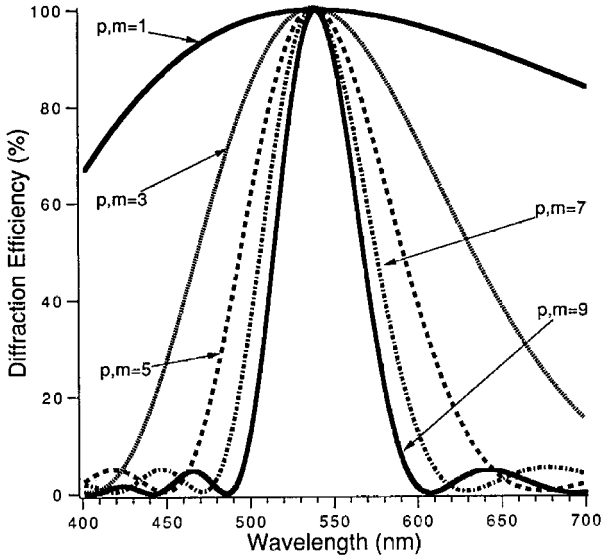

Fig. 3. Diffraction efficiency as a function of wavelength for $p = m$.

The wavelength bandwidth of the diffraction efficiency around a given diffracted order narrows with increasing values of p [see Eq. (8) and Fig. 3].[1,11] Also note that the material dispersion [see Eq. (3)] is an important parameter that must be retained in a detailed optical design.

Using Eq. (9), one can choose the parameters p and m that can allow high diffraction efficiency for certain bands in a given spectrum. The center wavelength of each of these bands comes to a focus a distance F_0 behind the lens. In Section 3, the imaging performance of a MOD lens is investigated.

3. Image Quality of Multiorder Diffractive Lenses

In section 2, we have shown that a MOD lens offers the potential for several wavelength components of the incident spectrum to come to a common focus. As a result, the polychromatic performance of the MOD singlet will differ substantially from the typical diffractive lens operating in a single diffraction order. Using the diffractive lens transmission function given in Eq. (5), one finds it useful to calculate the OTF for the paraxial diffractive singlet as a function of wavelength. In the present calculation, we include only the effects of the wavelength-dependent defocus and not any higher-order aberrations. These aberrations can be accounted for by the inclusion of appropriate phase terms in the diffraction integrals.

The field distribution in the real focal plane is given by

$$U_{\mathrm{II}}(u, v; \lambda) = \frac{-i}{\lambda F_0}\iint_{-\infty}^{\infty} U_{\mathrm{I}}(x, y; \lambda) P(x, y; \lambda) \times \exp\left\{\frac{i\pi}{\lambda F_0}[(u - x)^2 + (v - y)^2]\right\} \mathrm{d}x\mathrm{d}y, \tag{10}$$

where (u, v) represent the coordinates in plane II located a distance F_0 away and $P(x, y)$ is the complex pupil function. Substituting Eq. (5) into Eq. (10) and assuming a unit-amplitude plane wave as the input gives

$$U_{\mathrm{II}}(u, v; \lambda) = \frac{-i \exp\left[\frac{i\pi}{\lambda F_0}(u^2 + v^2)\right]}{\lambda F_0} \sum_{m=-\infty}^{\infty} \times \exp[-i\pi(\alpha p - m)]\mathrm{sinc}(\alpha p - m) \times \iint_{-\infty}^{\infty} P(x, y; \lambda)\exp\left[\frac{-i\pi}{\lambda}\epsilon(x^2 + y^2)\right] \times \exp\left[\frac{-i2\pi}{\lambda F_0}(ux + vy)\right]\mathrm{d}x\mathrm{d}y, \tag{11}$$

where

$$\epsilon = \frac{1}{F_0}\left(\frac{m\lambda}{p\lambda_0} - 1\right). \tag{12}$$

From Eq (11), it can be seen that the magnitude of the quantity ϵ is related directly to the amount of defocus in plane II. If other aberrations were present, one could construct a generalized pupil function in Eq. (11) that includes the phase errors introduced by the aberrations. The OTF is given by the autocorrelation of the generalized pupil function, suitably normalized:

$$\mathrm{OTF}(f_x, f_y) = \frac{\iint_{-\infty}^{\infty} H\left(\xi + \frac{f_x}{2}, \eta + \frac{f_y}{2}\right) H^*\left(\xi - \frac{f_x}{2}, \eta - \frac{f_y}{2}\right)\mathrm{d}\xi\mathrm{d}\eta}{\iint_{-\infty}^{\infty} |H(\xi, \eta)|^2 \mathrm{d}\xi\mathrm{d}\eta}, \tag{13}$$

where H represents the coherent transfer function of the system. If a rectangular pupil is assumed for simplicity[16] and Eq. (11) is used, the OTF is given by

$$\mathrm{OTF}(f_x, f_y) = \Lambda\left(\frac{f_x}{2f_0}\right)\Lambda\left(\frac{f_y}{2f_0}\right) \sum_{m=-\infty}^{\infty} \mathrm{sinc}^2(\alpha p - m) \times \mathrm{sinc}\left[\frac{\epsilon l^2}{\lambda}\left(\frac{f_x}{2f_0}\right)\left(1 - \frac{|f_x|}{2f_0}\right)\right] \times \mathrm{sinc}\left[\frac{\epsilon l^2}{\lambda}\left(\frac{f_y}{2f_0}\right)\left(1 - \frac{|f_y|}{2f_0}\right)\right], \tag{14}$$

where l is the diameter of the pupil aperture and

$$f_0 = \frac{l}{2\lambda F_0} \tag{15}$$

represents the cutoff frequency. In the derivation of Eq. (14) with Eq. (13), the cross terms in the double summation vanish because of an orthogonality condi-

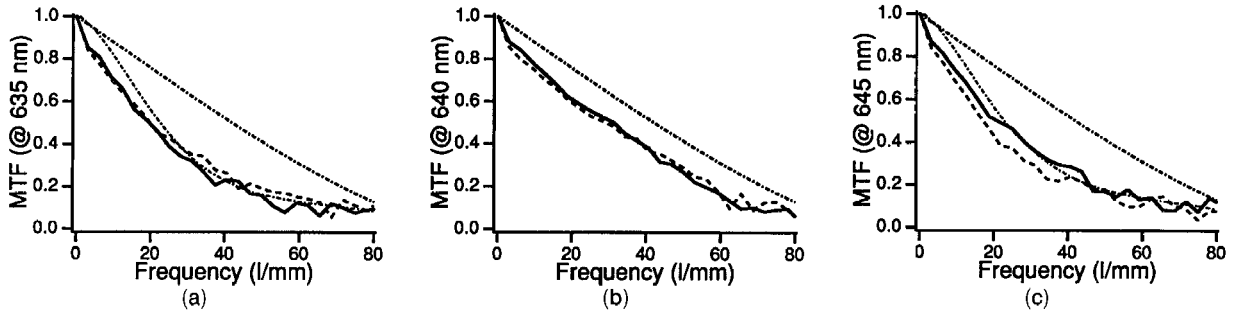

Fig. 4. MTF for $p = 2$ and $m = 2$. The design wavelength, 640 nm, is represented in (b) and a wavelength detuning of ±5 nm is represented in (a) and (c). The diffraction limit is the same in all three cases. The tangential MTF is displayed by a dashed curve, and the sagittal MTF is illustrated by a solid curve. The theoretical tangential performance at 635 and 645 nm is also illustrated as a dotted–dashed curve.

tion for the diffracted orders.[17] With reference to Eq. (14), note that for the cases in which $p = m = \alpha = 1$, and when $p = m$ and $\alpha = 1$, the OTF reduces to

$$\mathrm{OTF}(f_x, f_y) = \Lambda\left(\frac{f_x}{2f_0}\right)\Lambda\left(\frac{f_y}{2f_0}\right), \tag{16}$$

which represents the diffraction-limited OTF associated with a rectangular aperture. That is, the MOD lens provides for excellent imaging centered over a discrete set of wavelengths. For wavelength detunings [i.e., Eq. (7)], as we see in Section 4, the imaging performance is generally degraded and is dependent on p. Another figure of merit can be computed with the definition of the Strehl ratio given by

$$D = \frac{\displaystyle\int\int_{-\infty}^{\infty} \mathrm{OTF}(f_x, f_y)|_{\mathrm{aberrated}}\,\mathrm{d}f_x\mathrm{d}f_y}{\displaystyle\int\int_{-\infty}^{\infty}\left[\frac{\mathrm{OTF}(f_x, f_y)|_{\mathrm{unaberrated}}}{\displaystyle\sum_{m=-\infty}^{\infty}\mathrm{sinc}^2(\alpha p - m)}\right]\mathrm{d}f_x\mathrm{d}f_y}. \tag{17}$$

Because the diffraction of light into other orders reduces the OTF at the design order, the present definition of the Strehl ratio accounts for the nonunity diffraction efficiency. It is easily shown that the denominator of Eq. (17) is equal to $(2f_0)^2$. The Strehl ratio can now be rewritten as

$$D = \frac{1}{4f_0^2}\sum_{m=-\infty}^{\infty}\mathrm{sinc}^2(\alpha p - m) \times\left[\int_{-\infty}^{\infty}\Lambda\left(\frac{f_x}{2f_0}\right)\mathrm{sinc}\left[\frac{\epsilon l^2}{\lambda}\left(\frac{f_x}{2f_0}\right)\left(1 - \frac{|f_x|}{2f_0}\right)\right]\mathrm{d}f_x\right]^2. \tag{18}$$

With reference to Eqs. (14) and (18), the imaging performance of a MOD lens is certainly affected by the diffraction efficiency of the element. Aberration terms can also be included, and various approximations (see Ref. 17) can be made to evaluate the OTF and the Strehl ratio. In Section 4, experiments are presented for a MOD lens operated at two wavelength bands.

4. Experimental Demonstration

To illustrate the spectral characteristics of a MOD lens, an optical element was designed and fabricated for operation in the visible at $p = 2$ and $m = 2, 3$. The design wavelength was chosen to be 640 nm, which gives a third-order wavelength of 427 nm. The lens diameter was chosen to be 4.0 mm, and the focal length was determined to be 60 mm for operation at $f/15$.

The lens was fabricated by a single-point LPG.[18]

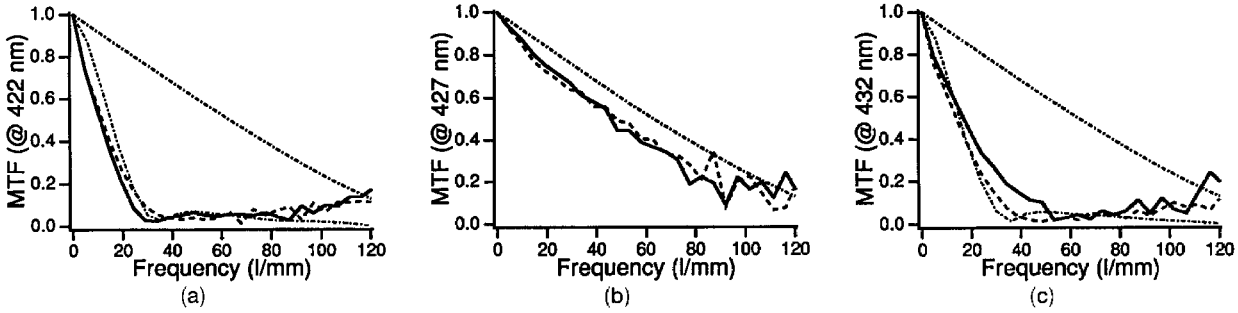

Fig. 5. MTF for $p = 2$ and $m = 3$. The design wavelength, 427 nm, is represented in (b) and a wavelength detuning of ±5 nm is represented in (a) and (c). The diffraction limit is the same in all three cases. The tangential MTF is displayed by a dashed curve, and the sagittal MTF is illustrated by a solid curve. The theoretical tangential performance at 422 and 432 nm is also illustrated as dotted–dashed curve.

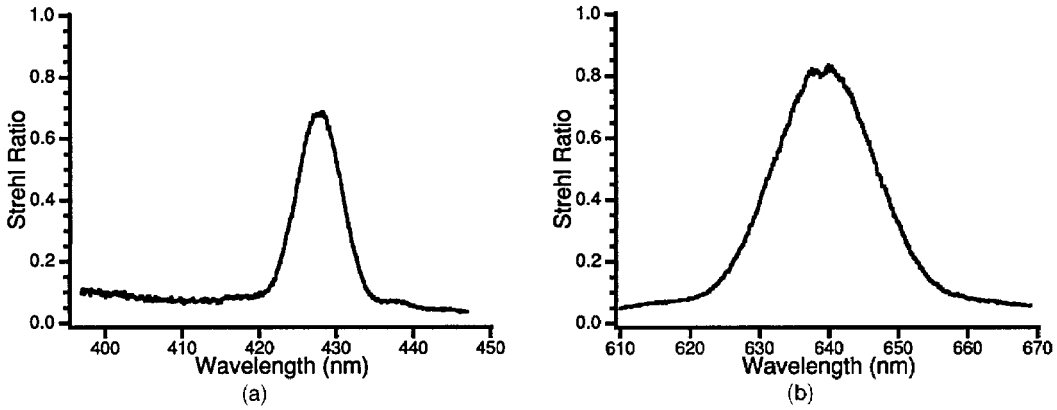

Fig. 6. Strehl ratio as a function of wavelength. The graph in (a) illustrates the performance at $p = 2$ and $m = 3$ and (b) at $p = 2$ and $m = 2$. Note that a Strehl ratio of 0.8 or greater denotes diffraction-limited performance.

The LPG uses a focused HeCd (i.e., $\lambda = 441$ nm) laser beam to expose photoresist in the linear portion of its exposure curve. During operation, the intensity of the laser is modulated so that 256 discrete phase levels can be recorded in the photoresist. The photoresist-coated substrate translates in the focal plane of the focusing lens; a high-bandwidth autofocus mechanism maintains a fixed focus position. The desired optical design data are integral to the LPG controller and are used to determine the intensity modulation of the laser source so that a blazed diffractive lens of the correct dimension is transferred into the photoresist. After the exposure process is complete, the photoresist is developed to give rise to a deterministic surface-relief diffractive lens. This master element can then be used as the basis of a process to fabricate replica elements. For this particular case, the integrated diffraction efficiency of the element was measured to be 91% for $m = 2$ and 3 by a diffraction efficiency test bed that provides for measurements over the entire visible band.

To illustrate the performance of the MOD lens in a specific diffracted order, the modulation transfer function (MTF) was measured with a broadly tunable MTF test bed. The MTF bench uses a source of tunable visible light to test lenses as a function of wavelength and field of view. In the usual manner, the edge-spread function is measured and used to give rise to the MTF in both sagittal and tangential meridians simultaneously. Figure 4 is a series of graphs that illustrates the MTF as a function of wavelength at $m = 2$ and at ± 5 nm from the design wavelength. Note that the performance is practically diffraction limited at the design wavelength and that the wavelength-dependent defocus degrades performance for detuned wavelengths. Equation (14) describes the reduction in image contrast for wavelengths other than the design wavelength. Figure 5 is another series of illustrations that displays the MTF as a function of wavelength for $m = 3$. Again the performance at the design wavelength is nearly diffraction limited. As an additional note, fabrication tolerances associated with the manufacture of MOD lenses (e.g., relief depth) become a more critical factor in the prediction of optical performance [see Fig. 3].

As described above, the Strehl ratio can also be used as a single-number figure of merit. The test bed was reconfigured to measure encircled energy in the Airy disk as a function of wavelength in the two wavelength bands near $m = 2$ and 3. This measurement was normalized[19] by the intensity of a perfect Airy disk to give a close approximation to the idealized Strehl ratio. The Strehl ratio is plotted in Fig. 6, with $m = 3$ depicted in Fig. 6(a) and $m = 2$ displayed in Fig. 6(b). Note that at the design wavelength, the performance is again measured to be near diffraction limited. For wavelength detunings, the Strehl ratio tends toward 0, which again results from the wavelength-dependent defocus.

5. Summary and Conclusions

MOD lenses offer the optical system designer a new element with interesting and useful spectral properties. We have shown that the first-order properties of the MOD lens allows the design of achromatic and apochromatic diffractive singlets; this property can be extremely useful for applications such as color projection displays and hyperspectral imaging. It was also shown [see Eq. (14)] that the OTF is highly wavelength dependent so that wavelength detunings from the design wavelength(s) cause reductions in the image contrast. Experiments were performed for the case of a MOD singlet with $p = 2$ and $m = 2, 3$. The performance of the lens was illustrated by MTF and Strehl measurements [see Figs. 4–6].

In general, the MOD lens will have different wavelength-dependent aberration properties from the conventional diffractive singlet (i.e., $p = 1$). However, there are cases, such as the diffractive landscape lens,[20] in which the third-order aberration properties of the MOD lens are identical to those found for the conventional wide-field diffractive singlet. A MOD landscape lens will have no third-order coma, astigmatism, and Petzval curvature for each wavelength that satisfies the equation $m = p\lambda_0/\lambda$; hence a MOD lens is able to provide high-quality imaging in broadband or multispectral illumination over wide fields of view.

In addition, this particular MOD lens has the required characteristics for a high-performance, multicolor laser scan lens and Fourier-transform lens.

The authors thank Stephen K. Mack for his assistance in the fabrication and testing of the multiorder diffractive lens.

References

1. K. Miyamoto, "The phase Fresnel lens," J. Opt. Soc. Am. **51,** 17–20 (1961).
2. D. Faklis and G. M. Morris, "Optical design with diffractive lenses," Photon. Spectra. **25**(11), 205–208 (1991).
3. P. P. Clark and C. Londono, "Production of kinoforms by single point diamond machining," Opt. News **15,** 39–40 (1989); J. A. Futhey, "Diffractive bifocal intraocular lens," in *Holographic Optics: Optically and Computer Generated,* I. Cindrich and S. H. Lee, eds. Proc. Soc. Photo-Opt. Instrum. Eng. **1052,** 142–149 (1989); G. M. Morris and D. A. Buralli, "Wide field diffractive lenses for imaging, scanning, and Fourier transformation," Opt. News **15,** 41–42 (1989).
4. L. d'Auria, J. P. Huignard, A. M. Roy, and E. Spitz, "Photolithographic fabrication of thin film lenses," Opt. Commun. **5,** 232–235 (1972); G. J. Swanson and W. B. Veldkamp, "Diffractive optical elements for use in infrared systems," Opt. Eng. **28,** 605–608 (1989).
5. D. Faklis and G. M. Morris, "Diffractive lenses in broadband optical system design," Photon. Spectra, **25**(12), 131–134 (1991).
6. G. M. Morris and D. Faklis, "Achromatic and apochromatic diffractive singlets," in *Diffractive Optics,* Vol. 11 of 1994 OSA Technical Digest Series (Optical Society of America, Washington, D.C., 1994), pp. 53–56.
7. H. Dammann, "Color separation gratings," Appl. Opt. **17,** 2273–2279 (1978).
8. H. Dammann, "Spectral characteristics of stepped-phase gratings," Optik **53,** 409 (1979).
9. J. A. Futhey, "Diffractive lens," U.S. Patent 4,936,666, (26 June 1990).
10. J. A. Futhey, M. Beal, and S. Saxe, "Superzone diffractive optics," in *Annual Meeting,* Vol. 17 of 1991 OSA Technical Digest Series (Optical Society of America, Washington, D.C., 1991), paper TuS2.
11. J. C. Marron, D. K. Angell, and A. M. Tai, "Higher-order kinoforms," in *Computer and Optically Formed Holographic Optics,* I. Cindrich and S. H. Lee, eds., Proc. Soc. Photo-Opt. Instrum. Eng. **1211,** 62–66 (1990).
12. D. W. Sweeney and G. Sommargren, "Single element achromatic diffractive lens," in *Diffractive Optics,* Vol. 11 of 1994 OSA Technical Digest Series (Optical Society of America, Washington, D.C., 1994), pp. 26–29.
13. D. B. Judd and G. Wyszecki, *Color in Business, Science and Industry* (Wiley, New York, 1975).
14. D. A. Buralli, G. M. Morris, and J. R. Rogers, "Optical performance of holographic kinoforms," Appl. Opt. **28,** 976–983 (1989).
15. J. W. Goodman, *Introduction to Fourier Optics* (McGraw-Hill, New York, 1968).
16. Ref. 15, Chap. 6, Eq. (6-37).
17. D. A. Buralli and G. M. Morris, "Effects of diffraction efficiency on the modulation transfer function of diffractive lenses," Appl. Opt. **31,** 4389–4396 (1992).
18. J. P. Bowen, C. G. Blough, and V. Wong, "Fabrication of optical surfaces by laser pattern generation," in *Optical Fabrication and Testing,* Vol. 13 of 1994 OSA Technical Digest Series (Optical Society of America, Washington, D.C., 1994), pp. 153–156.
19. W. J. Smith, *Modern Lens Design* (McGraw-Hill, New York, 1992), p. 44.
20. D. A. Buralli and G. M. Morris, "Design of diffractive singlets for monochromatic imaging," Appl. Opt. **30,** 2151–2158 (1991).